

from the analogous dependence for charged particle production.

### References

1. N.S.Amaglobeli et al. JINR, E1-9817, Dubna, 1976.
2. N.Angelov, V.G.Grishin, P.Kerachev.Yad.Fiz., 21, (1975) 1298.
3. N.S.Amaglobeli et al. JINR, E1-9820, Dubna, 1976.
4. A.J.Buras, J.Dias de Deus, R.Møller. Phys. Lett., 47B (1973) 251; A.Bassetto, J.Dias de Deus. Lett. Nuovo Cim., 9 (1974) 525.
5. N.S.Amaglobeli et al. JINR, P1-9847, Dubna, 1976.
6. Yu.A.Budagov et al. Paper 810/A2-110 presented to this Conference; to be published in Czech.Journ.Phys.B.
7. Yu.A.Budagov et al. JINR, E1-9501, Dubna, 1976.
8. N.S.Amaglobeli et al. JINR, E1-9854, Dubna, 1976.
9. N.S.Amaglobeli et al. Yad.Fiz., 22 (1975) 1269.

### NET CHARGE DISTRIBUTION IN RAPIDITY AND TRANSVERSE MOMENTUM FOR SEMI-INCLUSIVE $\pi^-p$ INTERACTIONS AT 11.2 GeV/c

(Bologna, Firenze, Genova, Milano, Oxford, Pavia Collaboration)

S.P.Ratti\* - Istituto di Fisica Nucleare and Sezione I.N.F.N. - Pavia (Italy)

We present an analysis of the net charge density distributions in  $\pi^-p$  collisions at 11.2 GeV/c, studying how electric charge gets distributed, for different topologies, as a function of rapidity  $Y$  and transverse momentum  $p_T$ . Following the notations of previous papers<sup>1,2/</sup> we define:

$$\rho_n(\vec{p}) = \frac{1}{N^n} \left\{ \frac{dN^{(+)}(\vec{p})}{d\vec{p}} - \frac{dN^{(-)}(\vec{p})}{d\vec{p}} \right\} = \rho_n^{(+)}(\vec{p}) - \rho_n^{(-)}(\vec{p}), \quad (1)$$

where  $n$  is the topology,  $dN^{(+,-)}(\vec{p})/d\vec{p}$  is the number of positive (negative) particles produced in a given interval of any kinematical variable  $\vec{p}$  (in our case;  $Y$  and  $p_T$ ) and  $N^n$  is the total number of events of a given topology.

The experimental data have been collected in a  $\approx 850.000$  picture exposure of the CERN 2m HBC exposed at the CERN PS to a  $\pi^-$  beam of 11.2 GeV/c. A total of 49593 two prongs, 107173 four prongs and 36656 six prongs is used. When necessary, proton tracks have been identified with a method developed by our collaboration<sup>3,4/</sup>.

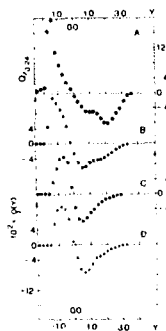


Fig.1. Charge density distributions  $\rho(Y; A)$  two prongs; B) four prongs; C) six prongs; D) cut four prongs  $t' > 0.4$  (GeV/c)<sup>2</sup>.

\* Co-authors are: R.Attendoli, E.Calligarich, G.Cecchet, R.Dolfini, L.Mapelli (Pavia); A.Quareni-Vignudelli (Bologna); S.Berti, A.M.Cartacci (Firenze); G.Tomasini, U.Trevisan (Genova); G.Costa, L.Perini (Milano); D.Radojicic, G.Thompson (Oxford).

The charge density distributions in rapidity  $\rho(Y)$  are shown in figs. 1a,b,c. The data show structures which were not clearly seen in previous similar analyses<sup>/1,2,5/</sup>. The sharp peak in positive charge excess at  $Y \approx -1.3$  in two prongs becomes, with increasing topology, broader and smaller. For six prongs, the position of the maximum shifts at  $Y \approx -0.7$ . In the region of  $Y > 0$ , an interesting effect is present in two and four prongs but not in six prongs. In figs. 1a and 1b, two minima are visible around  $Y_1 \approx 0.8$  and  $Y_2 \approx 2.4$ . The contributions to the two accumulations are however of different importance. In fig. 1a the excess at  $Y_1$  is  $\rho_1 \approx 5\%$  and at  $Y_2$  is  $\rho_2 \approx 8\%$ , while the opposite occurs in fig. 1b. The charge excess in six prong at  $Y_1$  (fig. 1c) is  $\rho_1 \approx 8\%$ . A similar behaviour could be seen in ref. (1) for  $\pi\bar{p}$  data, but there the topologies were added and, as a result, the effect is smeared out.



Fig. 2. Charge density distributions  $\rho(\rho_T)$ ; A) two prongs; B) four prongs; C) six prongs; D) cut four prongs  $t' > 0.4$  (GeV/c)<sup>2</sup>.

The distributions of  $\rho(\rho_T)$  are shown in figs. 2a,b,c. Again, they display topology dependent structures (positive excess at small  $\rho_T$  in two and four prongs, no positive excess in two prongs for  $\rho_T \geq 0.4$  GeV/c).

In figs. 3a,b,c the distributions of the charge density  $\rho(Y, \rho_T)$  are shown by means of equal-level curves:  $10^2 \cdot \rho(Y, \rho_T) = 0.0; 0.4; 0.8; \dots$  in units  $Q/c$  (0.08 GeV/c x 0.24). The structures, whose presence was detected in figs. 1a,b, become clear and separated. On the line of the most probable transverse momentum ( $\rho_T \approx 0.25$  GeV/c), peaks in charge excess are well visible. The position of the positive charge excess for six prongs at a smaller  $|Y|$  (fig. 3c) is due to the

multiplicity and to the presence of the massive nucleon. The splitting of the accumulation in  $\rho_T$ , is a consequence of the following facts; the  $\rho_T$  distributions are slightly different for protons and for negative pions<sup>/6,7/</sup>; the total negative charge  $Q = -3$  is large in six prongs; the position in  $Y$  of the positive excess in six prongs is much nearer to  $Y = 0$  than in two and four prongs<sup>/6/</sup>. In figs. 3a and 3b, the positive excess ( $\approx 0.8\%$ ) has similar extension and the same position. The relative importance of the two negative excesses for  $Y > 0$  (e.g. at the level of  $\approx -0.8\%$ ) is clearly seen from the figures.

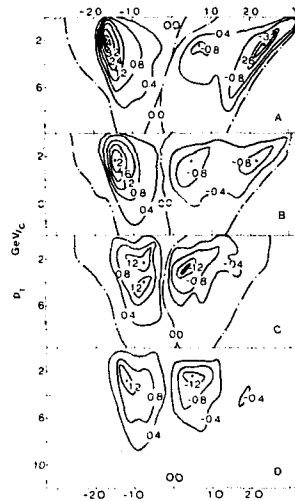


Fig. 3. Charge distributions  $\rho(Y, \rho_T)$ . Equal-level curves; A) two prongs; B) four prongs; C) six prongs; D) cut four prongs  $t' > 0.4$  (GeV/c)<sup>2</sup>.

An appealing explanation of the observed complex structures is the leading particle effect and/or diffraction dissociation, present in two and four prongs, but not in six prongs, at our energy.

To investigate this point we have performed several cuts and selections on both two and four prong events. For the sake of brevity, we show how a very simple cut on four prongs supports this explanation. In fact, by selecting  $t' > 0.4$  (GeV/c)<sup>2</sup> (where  $t' = t'_{beam, (3\pi)^-}$ ) all distributions of the four prong events are reduced identically to those of the six prong topology (apart from the splitting in  $\rho_T$  of the positive excess).

For cut four prong events  $\rho(Y)$  is shown in fig.1d;  $\rho(p_T)$  in fig.2d and  $\rho(Y, p_T)$  in fig.3d. The cut antiselects about 40% of the four prongs (61670 events surviving). The negative excess at  $Y_2$  disappears both in fig.1d and in fig.3d; the positive excess at small  $p_T$  in fig.2d is absent and the figures can be directly superimposed to figs.1c, 2c and 3c respectively. A similar procedure can be applied to the two prong events.

#### References

1. U.Idschok et al. Nuclear Phys. B67,93(1973).
2. T.Ferbel.U. of R. preprint COO-3065-91 (1974).
3. A.Forino et al.Nuovo Cimento 31A,696(1976).
4. A.Quareni-Vignudelli et al.Paper submitted to this Conference.
5. E.K.Kladnitskaya et al. Paper n.163 to this Conference.
6. P.Borzatta et al. Nuovo Cimento 15A,45(1973).
7. e.g. see M.Siansky. Physics Reports 11C,100 (1974).

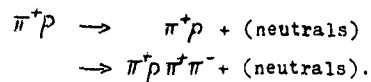
#### A SEARCH FOR NEW NEUTRAL PARTICLES PRODUCED IN HIGHLY INELASTIC $\pi^+$ PROTON COLLISIONS AT 10.5 GEV/C

J.R.Elliott, I.R.Fortney, A.T.Goshaw, J.W.Lamsa, J.S.Loos, W.J.Robertson, W.D.Walker, W.M.Yeager  
Physics Department, Duke University, Durham, North Carolina 27706

C.R.Sun, S.Dhar  
Physics Department, State University of New York, Albany, New York 12222

In recent years, detailed inclusive studies have been made of the charged particle spectrum coming from high energy hadronic interactions. In contrast, many simple but basic properties of the neutral particle spectrum still remain unexplored. We have done an experiment which makes an analysis of the neutral particle spectrum coming from 10.5 GeV/c  $\pi^+$  proton interactions in which a large fraction of the available energy goes into neutrals. The experiment is designed to determine if all the energy carried away by neutral particles can be accounted for by photons,  $K^0$ 's,  $\Lambda^0$ 's and neutrons. It uses the  $4\pi$  solid angle detection properties of a bubble chamber and has two distinct advantages over most other neutral particle searches. First, it is sensitive to new neutral particles produced in multineutral final states (in contrast to missing mass experiments). In addition, it does not rely upon any particular decay characteristics of the neutral particle.

The data were taken from an exposure of the SLAC 82" bubble chamber filled with a hydrogen-neon mixture (30 molar percent neon) and exposed to a 10.5 GeV/c  $\pi^+$  beam. We select 2 and 4 prong events with one identified proton and net-charge +2. This event sample consists of both neon and hydrogen interactions with about 65% of the events being free proton collisions. These are dominated by the processes



The event distribution as a function of the lon-